

Laser-driven hole boring and gamma-ray emission in high-density plasmas

E. N. Nerush* and I. Yu. Kostyukov

*Institute of Applied Physics of the Russian Academy of Sciences,
46 Ulyanov St., Nizhny Novgorod 603950,
Russia
University of Nizhny Novgorod,
23 Gagarin Avenue,
Nizhny Novgorod 603950,
Russia*

(Dated: June 28, 2021)

Ion acceleration in laser-produced dense plasmas is a key topic of many recent investigations thanks to its potential applications. Indeed, at forthcoming laser intensities ($I \gtrsim 10^{23} \text{ W cm}^{-2}$) interaction of laser pulses with plasmas can be accompanied by copious gamma-ray emission. Here we demonstrate the mutual influence of gamma-ray emission and ion acceleration during relativistic hole boring in high-density plasmas with ultra-intense laser pulses. If the gamma-ray emission is abundant, laser pulse reflection and hole-boring velocity are lower and gamma-ray radiation pattern is narrower than in the case of low emission. Conservation of energy and momentum allows one to elucidate the effects of the gamma-ray emission which are more pronounced at higher hole-boring velocities.

I. INTRODUCTION

Starting from the pioneering papers of Wilks and Denavit (Denavit, 1992; Wilks *et al.*, 1992), showing that relativistically intense laser pulses can bore holes in overdense plasmas and accelerate ions by the radiation pressure, the radiation pressure acceleration has been intensively studied and discussed. E.g., the radiation pressure acceleration was investigated in recent experiments (Kar *et al.*, 2013; Palmer *et al.*, 2011), relativistic hole boring was studied theoretically (Robinson *et al.*, 2009; Schlegel *et al.*, 2009) and proposed for fast ignition schemes (Naumova *et al.*, 2009), it is shown by means of numerical simulations that the radiation pressure acceleration is feasible for acceleration of ions up to GeV energies (Esirkepov *et al.*, 2004; Ji *et al.*, 2014a), see also Ref. (Macchi *et al.*, 2013).

A number of planned laser facilities (Bashinov *et al.*, 2014; Mourou and Tajima, 2014) aim to reach high field intensity in order to demonstrate a plenty of novel phenomena such as electromagnetic cascades (Bell and Kirk, 2008; Fedotov *et al.*, 2010; Nerush *et al.*, 2011a), vacuum birefringence (King and Di Piazza, 2014), and electron-positron pair creation (Narozhny and Fedotov, 2014). Besides these effects requiring special set-ups (Bashmakov *et al.*, 2014; Gonoskov *et al.*, 2013) a number of rough phenomena should occur. E.g., incoherent synchrotron emission of hard photons will be an inherent feature of extremely relativistic plasma physics (Ji *et al.*, 2014c; Nakamura *et al.*, 2012; Nerush *et al.*, 2014; Ridgers

et al., 2012). The latter phenomenon should surely affect particle dynamics in the laser-driven hole boring.

Here we study the hole boring in high-density plasmas accompanied by gamma-ray emission. A relativistic laser pulse (intensity $I \gtrsim 10^{18} \text{ W cm}^{-2}$ for optical wavelengths) can drive plasmas by its front (Wilks *et al.*, 1992). The laser field pushes plasma electrons which sweep ions by a longitudinal electric field in a thin shock-like layer of charge separation (Macchi *et al.*, 2005; Schlegel *et al.*, 2009). Some properties of the process (front velocity, ion energy, etc.) can be found using momentum and energy conservation laws in the nonrelativistic (Kruer *et al.*, 1975; Wilks *et al.*, 1992) and in the relativistic cases (Naumova *et al.*, 2009; Robinson *et al.*, 2009), and measured in the experiments (Kar *et al.*, 2013). If the laser intensity is $I \gtrsim 10^{23} \text{ W cm}^{-2}$, plasma electrons can efficiently emit high-energy photons.

One- and two-dimensional simulations with radiation reaction force taken into account show that the radiation losses decrease the hole-boring velocity, suppress the filamentation process and affect the electron and ion distributions (Capdessus *et al.*, 2012; Naumova *et al.*, 2009; Schlegel *et al.*, 2009; Tamburini *et al.*, 2010). It is generally believed that radiation losses do not affect radiation pressure acceleration much if circularly polarized pulses are used (particularly for thin targets) (Chen *et al.*, 2011; Tamburini *et al.*, 2012, 2010). However, here we show that if laser intensity is extremely high, $I \sim 10^{25} \text{ W cm}^{-2}$, high-energy photons can take away a great portion of laser energy at least for thick targets (generation of hard photons in this case can be stimulated by pair production, see Sec. IV).

The approach that uses the radiation reaction force doesn't take into account quantum nature of photon

* nerush@appl.sci-nnov.ru

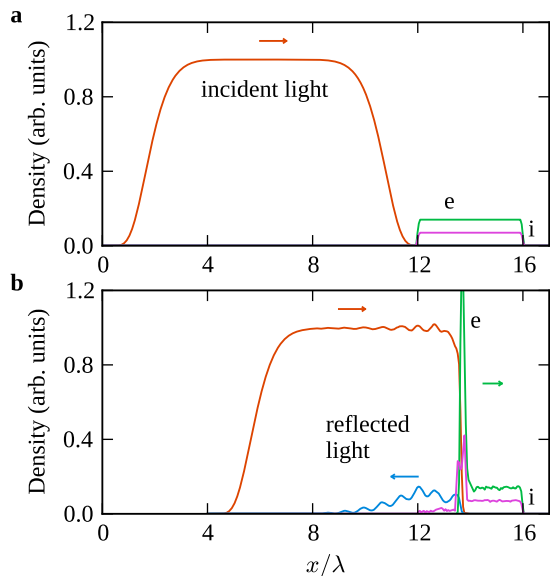


FIG. 1 On-axis shape of the incident (orange) and reflected (blue) laser pulses, electron density (green) and ion density (violet) in a particle-in-cell simulation at time instances $t = 0$ (a) and $t = 4\lambda/c$ (b).

emission that is important in some cases (Duclous *et al.*, 2011; Nerush and Kostyukov, 2011). Moreover, radiation losses in quantum regime (when quantum recoil is significant) cannot be described by the concept of a classical force in principle (Elkina *et al.*, 2011).

Here we use the three-dimensional PIC code with emission of hard photons taken into account by means of Monte Carlo method (Nerush *et al.*, 2014). Electron-positron pair production (photon decay) is also taken into account that allows us simulate the hole boring process at intensities about $10^{25} \text{ W cm}^{-2}$ and higher. Similar approach has been used in a number of articles (Brady *et al.*, 2014; Ridgers *et al.*, 2013, 2012) where absence of reflection, the modification of the ion spectrum and the influence of gamma-ray emission on the energy budget are mentioned. However, the influence of incoherent emission on the hole boring was not the main topic of these articles and was not covered in details.

Here we present detailed results of numerical simulations and theoretical analysis that takes into account radiation losses during the laser-driven hole boring and elucidates the key effects of gamma-ray emission.

II. CONSERVATION OF ENERGY AND MOMENTUM IN LASER-PLASMA INTERACTIONS

To investigate the influence of gamma-ray generation on ion acceleration we consider the interaction geometry where a laser pulse is incident on a plasma slab producing reflected light, ion flow and high-energy photons

(Fig. 1). According to Ref. (Ji *et al.*, 2014c), the ratio of the electron energy to the overall energy in laser-plasma interactions decreases as the intensity increases, and for $I \gtrsim 10^{23} \text{ W cm}^{-2}$ the electron energy can become negligible in the energy balance. Therefore, conservation of energy and momentum is given as:

$$(1 - R)S_l = S_i + S_\gamma, \quad (1)$$

$$(1 + R)S_l = \Pi_i + S_\gamma \cos \varphi_0, \quad (2)$$

where S_l , S_i and S_γ are the laser pulse energy, the overall ion energy and the overall energy of gamma-rays, respectively, Π_i/c is the overall ion momentum, $\cos \varphi_0$ determines the ratio of the longitudinal momentum of gamma-rays to their energy (i.e., φ_0 is the halfangle of the gamma-ray divergence), R is the reflection coefficient and c is the speed of light. It follows from Eqs. (1)-(2) that

$$\Pi_i - S_i = 2RS_l + (1 - \cos \varphi_0)S_\gamma, \quad (3)$$

$$\Pi_i + S_i = 2S_l - (1 + \cos \varphi_0)S_\gamma. \quad (4)$$

If $\Pi_i = 0$, Eq. (3) is fulfilled only in the unrealistic case of $R = 0$, $S_i = 0$ and $\varphi_0 = 0$. This means that Π_i should be greater than zero, hence the gamma-ray generation is always accompanied by ion acceleration.

In addition, when the ion acceleration is accompanied by gamma-ray emission, the former should be affected by the latter according to the momentum end energy conservation. The effect of gamma-ray emission is quite simple if the ions are ultrarelativistic.

In laser-foil interactions ions gain velocity almost equal to the speed of light, for instance, in the laser-piston regime (Esirkepov *et al.*, 2004). In this regime light pressure pushes a foil behaving as a mirror. The reflection coefficient tends to zero due to relativistic motion of the foil (Esirkepov *et al.*, 2004), and gamma-rays are emitted primarily in the forward direction ($\varphi_0 \simeq 0$) because of light aberration and relativistic Doppler effect (Nerush *et al.*, 2014; Ridgers *et al.*, 2012). These features of laser-plasma interaction apparently are also inherent for ultrarelativistic hole-boring. Furthermore, for ultrarelativistic ions $\Pi_i \simeq S_i$, hence Eq. (3) is naturally fulfilled, and Eq. (4) yields $S_i \simeq S_l - S_\gamma$. Therefore, the gamma-ray emission just lowers the ion acceleration rate if ions are ultrarelativistic.

III. ENERGY AND MOMENTUM BALANCE IN LASER-DRIVEN HOLE BORING

The laser-driven hole boring is a well-known interaction regime that can be roughly described as ion acceleration by a kick from a shock moving together with the laser pulse front with the speed v_{hb} (Robinson *et al.*, 2009; Schlegel *et al.*, 2009; Wilks *et al.*, 1992). Rebounded ions overtake the front and, since all of them move with the

same velocity v_r , they form a quasimonoenergetic distribution. In fact, ions in this regime are accelerated by the electric field induced by the laser pulse through electron-ion separation (Nerush *et al.*, 2014; Schlegel *et al.*, 2009). Every rebounded ion passes the same track in the field, hence, all of them gain the same energy. This idealized picture allows one to find the speed of the laser pulse front, v_{hb} , as demonstrated in Sec. III.A for almost absent gamma-ray emission and in Sec. III.B for abundant gamma-ray emission.

A. Low gamma-ray emission

The conservation laws Eqs. (1), (2) can be written not only for the overall energy and momentum, but also for the energy and momentum flow rates per unit area of the shock:

$$\frac{(1-R)(c-v_{hb})}{4\pi} |\mathbf{E} \times \mathbf{B}| = n_i v_{hb} M c^2 (\gamma_r - 1), \quad (5)$$

$$\frac{(1+R)(c-v_{hb})}{4\pi} |\mathbf{E} \times \mathbf{B}| = n_i v_{hb} M c v_r \gamma_r, \quad (6)$$

where \mathbf{E} and \mathbf{B} are electric and magnetic fields of the laser pulse, n_i is the initial ion density, M is the ion mass and $\gamma_r = c(c^2 - v_r^2)^{-1/2}$ is the Lorentz factor of the rebounded ions. It follows directly from these equations that

$$R = \sqrt{\frac{c-v_r}{c+v_r}}, \quad (7)$$

$$\frac{c-v_{hb}}{2\pi} |\mathbf{E} \times \mathbf{B}| = M c n_i v_{hb} [\gamma_r(c+v_r) - c]. \quad (8)$$

The velocity and the Lorentz factor of the accelerated ions can be found from the assumption of perfectly elastic rebound in the reference frame co-moving with the front of the laser pulse:

$$v_r = \frac{2c^2 v_{hb}}{c^2 + v_{hb}^2}, \quad \gamma_r = \frac{c}{\sqrt{c^2 - v_r^2}} = \frac{c^2 + v_{hb}^2}{c^2 - v_{hb}^2}. \quad (9)$$

From these equations together with Eqs. (7) and (8) we get, first, $R = (c - v_{hb}) / (c + v_{hb})$. This formula corresponds to a complete laser light reflection in the reference frame co-moving with the front of the laser pulse. Second,

$$v_{hb} = \frac{c}{1 + \mu}, \quad \mu = \sqrt{\frac{4\pi c^2 M n_i}{|\mathbf{E} \times \mathbf{B}|}} = \frac{1}{a_0} \sqrt{\frac{M n_i}{m n_{cr}}}, \quad (10)$$

that matches with the results obtained in Refs. (Robinson *et al.*, 2009; Schlegel *et al.*, 2009) by a slightly different approach. Here $n_{cr} = m\omega^2 / 4\pi e^2$ is the critical density, ω is the laser cyclic frequency, m and $e > 0$ are the electron mass and the electron charge magnitude, respectively, $a_0 = eE_0 / m c \omega$ is the normalized amplitude of the incident laser pulse, E_0 .

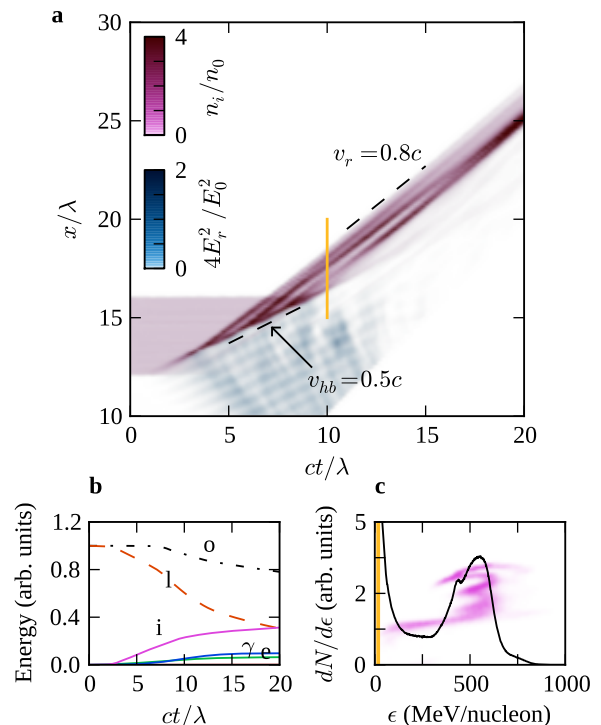


FIG. 2 The results of a numerical simulation of a circularly polarized laser pulse ($a_0 = 500$) in normal incidence on a $4 \mu\text{m}$ -thick He slab (initial ion density is $n_0 = 35n_{cr}$). (a) On-axis ion density normalized to the initial ion density and intensity of the reflected light; $E_r^2 = (\mathbf{E} - \mathbf{B} \times \mathbf{e}_0)^2 / 4$ is the squared electric field of the reflected wave, E_0 is the amplitude of the incident wave and \mathbf{e}_0 is the unit vector of the propagation direction of the incident pulse. (b) The overall, laser, ion and electron energy, and the energy of gamma-rays during the interaction. The decline in the overall energy corresponds to the exit of the reflected light from the simulation box. (c) Spectrum of all ions and the distribution of on-axis ions in the $\epsilon - x$ phase space at $t = 10\lambda/c$. Here $\epsilon = M c^2 (\gamma - 1)$ is the kinetic energy of an ion.

Results of a three-dimensional particle-in-cell simulation with incoherent emission taken into account illustrate well hole boring with an intense laser pulse in a dense plasma (Figs. 1, 2). The simulation box is $17.5\lambda \times 25\lambda \times 25\lambda$ corresponding to the grid size $670 \times 125 \times 125$ with the cell size $0.026\lambda \times 0.2\lambda \times 0.2\lambda$. The time step is $0.019\lambda/c$, where λ is the laser wavelength. The initial number of quasiparticles is 3.8×10^7 corresponding to 16 particles per cell in the unperturbed plasma. In the simulation a quasi-rectangular ($12\lambda \times 24\lambda \times 24\lambda$) circularly polarized laser pulse of intensity $7 \times 10^{23} \text{ W cm}^{-2}$ ($\lambda = 1 \mu\text{m}$, $a_0 = 500$) interacts with a He slab ($n_e = 2n_i = 7.8 \times 10^{22} \text{ cm}^{-3}$, $n_i/n_{cr} = 35$). Helium becomes fully ionized, then electrons are pushed by $\mathbf{v} \times \mathbf{B}$ force resulting charge separation that creates accelerating field. For the given parameters $\mu = 1$ and $v_{hb} = 0.5c$ that is in fairly good agreement with the nu-

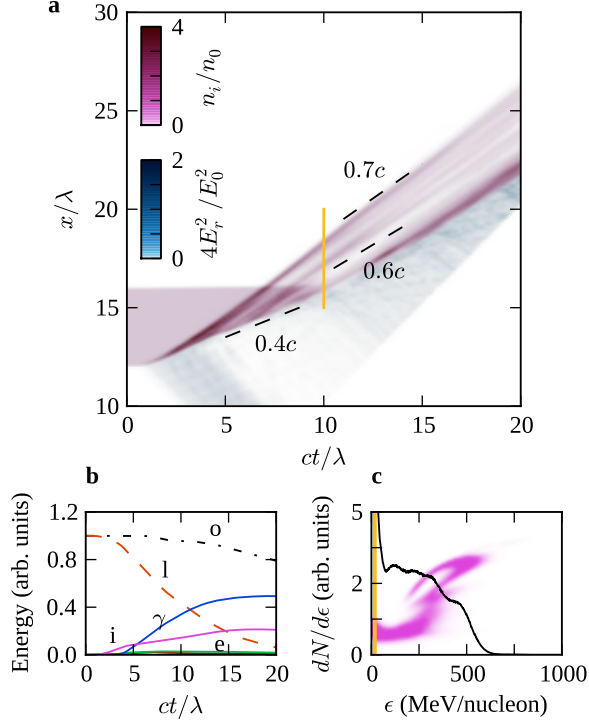


FIG. 3 The results of a numerical simulation of a circularly polarized laser pulse ($a_0 = 1840$) in normal incidence on a $4 \mu\text{m}$ -thick diamond foil (initial ion density is $n_0 = 158n_{cr}$). (a) On-axis ion density and intensity of the reflected light. The sharp front of the reflected field distribution at $t \gtrsim 10$ is caused by a boundary of the simulation box. (b) The overall, laser, ion and electron energy, and the energy of gamma-rays during the interaction. (c) Spectrum of all ions and the distribution of on-axis ions in $\epsilon - x$ phasespace at $t = 10\lambda/c$.

merical results [Fig. 2(a)]. The overall ion energy grows linearly with time while the laser pulse front is passing the slab [$3\lambda/c \lesssim t \lesssim 9\lambda/c$, see Fig. 2(b)]. However, the rebound of ions is not regular in time and the resulting ion spectrum is not strictly monoenergetic [Fig. 2(c); on the broadening of the ion spectrum and modulations in the phasespace see also Refs. (Macchi *et al.*, 2013; Robinson *et al.*, 2009; Schlegel *et al.*, 2009)].

B. Abundant gamma-ray emission

According to Eq. (10) that doesn't take into account high-energy photons, the hole-boring velocity remains the same if Mn_i (i.e. mass density) is increased proportionally to the laser intensity. If the hole-boring velocity is non-relativistic, the gamma-ray generation efficiency is low and doesn't grow with simultaneous increase of the intensity and the density (Nerush *et al.*, 2014). However, the energy taken away by gamma-rays increases sharply with the intensity and can be of the order of the initial laser pulse energy in the case of relativistic hole boring.

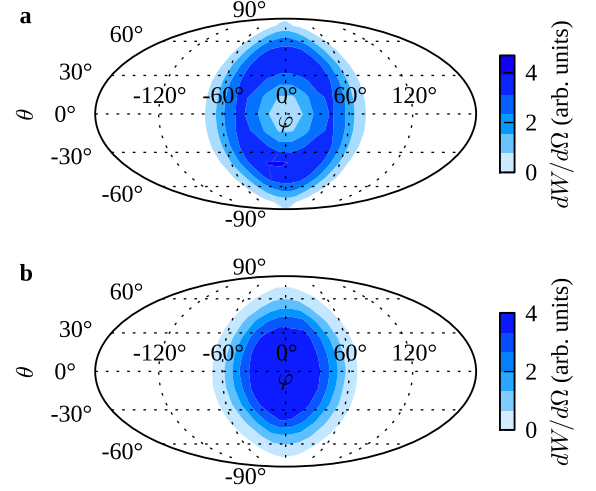


FIG. 4 The Mollweide projection of the gamma-ray radiation pattern, i.e. the angular distribution of the emitted energy, in normal incidence of a laser pulse ($a_0 = 1840$) on a $4 \mu\text{m}$ -thick diamond foil at $t = 5\lambda/c$ (a) and $t = 10\lambda/c$ (b). The longitude φ and the latitude θ are introduced so that the point $\varphi = 0$, $\theta = 0$ corresponds to the propagation direction of the incident laser pulse.

PIC simulation (Fig. 3; the simulation box is $17.5\lambda \times 25\lambda \times 25\lambda$, the cell size is $0.007\lambda \times 0.17\lambda \times 0.17\lambda$, the time step is $0.005\lambda/c$, the initial number of quasiparticles is 2×10^8 that is barely enough to resolve high-energy tails in the electron distribution, thus massive simulations are desirable in the future) shows that in the interaction of a $9.3 \times 10^{24} \text{ W cm}^{-2}$ ($a_0 = 1840$) laser pulse with a diamond foil ($n_e = 6n_i = 1.1 \times 10^{24} \text{ cm}^{-3}$, $n_i/n_{cr} = 158$) the fraction of energy carried away by gamma-rays is 2.3 times larger than that of ions [Fig. 3(b)]; in the previous case, for a He slab and a laser pulse of $a_0 = 500$, this ratio is only 0.3. Though μ is the same in both cases, such sizeable energy losses, caused by incoherent synchrotron emission in the second case, considerably affect the interaction process. Primarily, the reflection coefficient, the hole-boring velocity and the ion spectrum are involved.

To determine the effect of radiation losses we introduce them into Eqs. (5) and (6):

$$\frac{(1-R)(c-v_{hb})}{4\pi} |\mathbf{E} \times \mathbf{B}| = n_i v_{hb} M c^2 (\gamma_r - 1) + S_\gamma, \quad (11)$$

$$\frac{(1+R)(c-v_{hb})}{4\pi} |\mathbf{E} \times \mathbf{B}| = n_i v_{hb} M c v_r \gamma_r + S_\gamma \cos \varphi_0. \quad (12)$$

From these equations the reflection coefficient can be found as the function of the rebound speed v_r , the emission angle φ_0 and

$$\eta_{\gamma i} = S_\gamma / n_i v_{hb} M c^2 (\gamma_r - 1), \quad (13)$$

the fraction of the energy carried away by gamma-rays to the energy carried away by ions, as follows:

$$R = \sqrt{\frac{c-v_r}{c+v_r}} \frac{1 - (1 - \cos \varphi_0) \eta_{\gamma i} f^-}{1 + (1 + \cos \varphi_0) \eta_{\gamma i} f^+}, \quad (14)$$

$$f^\pm = \frac{1}{\sqrt{c \pm v_r}} \frac{c - \sqrt{c^2 - v_r^2}}{\sqrt{c + v_r} - \sqrt{c - v_r}}. \quad (15)$$

If gamma-ray emission is abundant, $\eta_{\gamma i} \gg 1$ (for instance, from the slope of the curves in Fig. 3(b) we obtain $\eta_{\gamma i} \simeq 5$). The function f^+ increases from 0 to 1/2 and the function f^- changes from 0 to ∞ if v_r grows from 0 to 1. Thus, if the hole-boring is relativistic, the products $\eta_{\gamma i} f^+$ and $\eta_{\gamma i} f^-$ become greater than unity and the reflection coefficient in this case tends to zero. Furthermore, if $\eta_{\gamma i} f^- \gg 1$, the gamma-rays are emitted mostly in the forward direction ($\cos \varphi_0 \simeq 1$), otherwise Eq. (14) yields $R < 0$. As f^+ and f^- increase with the increase of v_r , the decrease of the reflection coefficient and the narrowing of the gamma-ray radiation pattern caused by the radiation losses become more pronounced at higher hole-boring velocities.

The effects following from Eq. (14) are in fairly good agreement with the simulation results presented in Fig. 3. Most portion of gamma-rays are emitted at $5\lambda/c \lesssim t \lesssim 10\lambda/c$, and the reflection coefficient is very low during this time interval [Fig. 3(a)]. In addition, the gamma-ray radiation pattern at $t = 5\lambda/c$ is conical with $\varphi_0 \simeq 45^\circ$, and the radiation pattern at $t = 10\lambda/c$ is rather spotlight-like (Fig. 4). The difference between these patterns can be interpreted as follows. For $t \lesssim 5\lambda/c$ the gamma-ray generation efficiency is low, hence radiation losses do not affect the laser-plasma interaction much and conical radiation pattern is formed [the radiation pattern formed in the incidence of a laser pulse with $a_0 = 500$ on a He slab (see Sec. III.A) is almost the same]. Most part of gamma-rays is emitted during the time interval $5\lambda/c \lesssim t \lesssim 10\lambda/c$, that affects the laser-plasma interaction and leads to the narrowing of the gamma-ray radiation pattern [Fig. 4(b)].

We assume that when a laser pulse bores a hole in a plasma, a potential barrier is created at the front of the laser pulse in the case of abundant gamma-ray emission also. Rebound of ions from the moving potential barrier is elastic and, in the reference frame co-moving with the barrier, value of the ion velocity doesn't change after the rebound. Thus, in the laboratory reference frame the velocity of the laser pulse front and the velocity of the rebounded ions are related according to Eq. (9). Together with Eqs. (11)-(12) this yields:

$$\frac{(c - v_{hb})}{4\pi} |\mathbf{E} \times \mathbf{B}| = \frac{Mc^2 n_i v_{hb}^2}{c - v_{hb}} + \frac{S_\gamma (1 + \cos \varphi_0)}{2}, \quad (16)$$

and the velocity of the laser pulse front, v_{hb} , is deter-

mined by Eq. (10) with $\tilde{\mu}$ substituted for μ :

$$v_{hb} = \frac{c}{1 + \tilde{\mu}}, \quad \tilde{\mu} = \frac{\mu}{\sqrt{1 - \sigma_{\gamma l}}}, \quad (17)$$

$$\mu = \frac{1}{a_0} \sqrt{\frac{Mn_i}{mn_{cr}}}, \quad \sigma_{\gamma l} = \frac{2\pi(1 + \cos \varphi_0)S_\gamma}{(c - v_{hb})|\mathbf{E} \times \mathbf{B}|}. \quad (18)$$

At high radiation losses, when $R \simeq 0$ and $\cos \varphi_0 \simeq 1$, $\sigma_{\gamma l}$ is approximately equal to the gamma-ray generation efficiency, i.e., the ratio of the emitted gamma-ray energy, τS_γ , to the absorbed laser pulse energy, $\tau(c - v_{hb})|\mathbf{E} \times \mathbf{B}|/4\pi$, where τ is the interaction time. From the slope of the curves in Fig. 3(b) for $5\lambda/c \lesssim t \lesssim 10\lambda/c$ we obtain $\sigma_{\gamma l} \simeq 0.7$, hence Eqs. (17) and (9) yield $\tilde{\mu} = 1.8$, $v_{hb} = 0.36c$ and $v_r = 0.6c$ ($\epsilon = 270$ MeV/nucleon). These analytical results describes well ion dynamics in the numerical simulation (Fig. 3). However, the ion distribution in $\epsilon - x$ phase space consist not only of vertical part with $\epsilon \simeq 250$ MeV/nucleon, but also of parts with higher and lower energy. Fig. 3(a) demonstrates that ions with $v_r \gtrsim 0.6c$ are accelerated when the gamma-ray generation is not yet efficient ($t \lesssim 5\lambda/c$) and ions with $v_r \lesssim 0.6c$ are accelerated when the laser front leaves the foil that is accompanied by a decrease in the accelerating field ($t \simeq 10\lambda/c$). The amount of low-energy ions in the case of $a_0 = 500$ laser pulse and He slab (Sec. III.A) is much lower than in the considered case. This indicates, possibly, much longer acceleration time in the case of abundant emission. However, here we do not consider in detail how (from the microscopic point of view) efficient gamma-ray generation is connected with the decrease in ion acceleration rate and in reflection coefficient, and how it is connected with narrowing of the radiation pattern. We limit ourselves to demonstration of these general effects of gamma-ray emission.

IV. DISCUSSION

If the incoherent photon emission is absent, energy of a laser pulse that bores a hole in a dense plasma is transmitted mostly to ions and reflected light. In this case proportional increase of the laser intensity and the plasma mass density doesn't change the interaction pattern (hole-boring velocity, velocity of ions, etc.). However, at high intensities efficient generation of hard photons occurs that changes energy and momentum balances. First, as a great part of the laser energy is transmitted to hard photons, the energy of the reflected light drops together with the hole-boring velocity and the energy of rebounded ions. Second, the gamma-ray radiation pattern should be quite narrow and directed along the initial direction of the laser pulse, because a great part of the laser momentum is carried away by gamma-rays and is not taken away by the ions. We show that the drop in the reflection coefficient and the narrowing of the gamma-ray radiation pattern caused by the losses

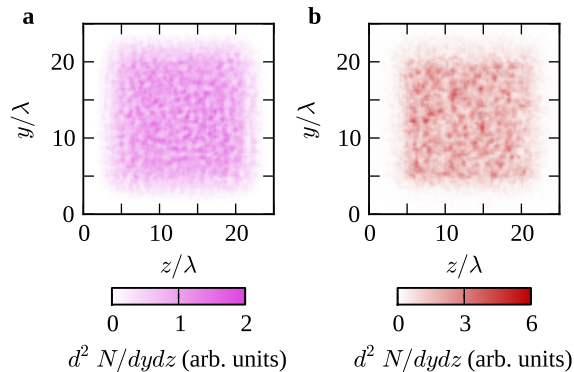


FIG. 5 Distribution of ions with $\epsilon > 250$ MeV/nucleon (a) and positrons along the plane of the shock generated in normal incidence of a circularly polarized laser pulse ($a_0 = 1840$) on a diamond foil. The distributions are normalized to the average value of the ion distribution.

are more pronounced for higher hole-boring velocities. In the opposite, the kinetic energy of the rebounded ions $\gamma_r - 1 = 2/(2\tilde{\mu} + \tilde{\mu}^2)$ is more sensitive to the radiation losses if $\tilde{\mu} \gg 1$, i.e. at low hole-boring velocities. Nonetheless, at high hole-boring velocities radiation losses also influence on the ion acceleration and can reduce the acceleration rate.

Three-dimensional particle-in-cell simulations with incoherent emission of hard photons and pair production taken into account agree well with the proposed picture that follows from the energy and momentum conservation laws. However, numerical simulations reveal a number of phenomena not taken into account by the analytical model. First, even in the case of low gamma-ray emission the beam of accelerated ions is not strictly homogeneous, and the ion spectrum is not strictly monoenergetic (Fig. 2). Second, in the ultrahigh-intensity case the ion acceleration rate changes with time leading to a broad ion spectrum (Fig. 3). The broadening of the ion spectrum in the low-emission case is caused by the piston oscillations (Macchi *et al.*, 2013; Robinson *et al.*, 2009; Schlegel *et al.*, 2009) that lead to the modulations in the phasespace [Fig. 2(c)] and modulations in the reflected light [Fig. 1(b)]. At the same time, the broad ion spectrum and modulations in the phasespace [Fig. 3(c)] in ultrahigh-intensity case are caused by the radiation losses that are correlated with pair production (see below).

The beam of the rebounded ions is propagating through the unperturbed plasma that causes Weibel-type instability and beam filamentation (Fox *et al.*, 2013), filamentation of the laser pulse front (Naumova *et al.*, 2009; Palmer *et al.*, 2012) also occurs. Filamentation of the ion beam and the laser pulse front is more pronounced in the case of low gamma-ray emission. In the given numerical simulations ion filaments have no time to coalesce,

however, for a thick foils filamentation of the ion flow and magnetic field generation can significantly change the ion distribution function, as happens in plasmas of gamma-ray burst outflows (Bret *et al.*, 2014; Silva *et al.*, 2003)

In the case of abundant gamma-ray emission hard photons decay and create electron-positron pairs in strong laser and plasma fields. Numerical simulations show that in the case of ultra-intense laser pulse pair production is crucial for efficient gamma-ray generation. For the simulation with $a_0 = 1840$ the number of produced positrons is about the initial number of electrons in the simulation box, and the number of hard photons produced by the positrons is about the number of hard photons produced by electrons. The possible explanation is that the generated positrons can stay near the shock for a long time and generate gamma-rays efficiently. If pair production is not included in PIC simulation, the gamma-ray generation efficiency, the hole boring velocity and the ion spectrum are close to that in the case of much less intense laser pulse ($a_0 = 500$) and He slab. Thus, the feedback between processes of quantum electrodynamics and plasma physics (Ji *et al.*, 2014b; Nerush *et al.*, 2011b; Ridgers *et al.*, 2013) is evident in this case. The positron dynamics during hole boring with ultra-intense laser pulses is studied in Ref. (Kirk *et al.*, 2013), however, a vacuum gap assumed there is absent in our simulations; moreover, filamentation of the positron beam occurs (Fig. 5). This indicates that further investigations are needed. Nevertheless, pair plasma does not directly involved in energy and momentum balances and just converts laser energy into gamma-ray energy. Hence, the analysis presented here is also valid in the case of abundant pair production.

In conclusion, the influence of radiation losses on a hole boring with ultra-intense laser pulses is considered by means of three-dimensional simulations and theoretical analysis. Conservation of momentum and energy allows one to understand how the losses affect hole boring properties for any mechanism of the incoherent photon emission.

ACKNOWLEDGMENTS

This work has been supported in part by the Government of the Russian Federation (Project No. 14.B25.31.0008) and by the Russian Foundation for Basic Research (Grants No 13-02-00886, 15-02-06079).

REFERENCES

- Bashinov, A. V., A. A. Gonoskov, A. V. Kim, G. Mourou, and A. M. Sergeev (2014), The European Physical Journal Special Topics **223** (6), 1105.
- Bashmakov, V. F., E. N. Nerush, I. Y. Kostyukov, A. M.

- Fedotov, and N. B. Narozhny (2014), *Physics of Plasmas* **21**, 013105.
- Bell, A., and J. Kirk (2008), *Physical Review Letters* **101** (20), 200403.
- Brady, C. S., C. P. Ridgers, T. D. Arber, and A. R. Bell (2014), *Physics of Plasmas* **21** (3), 033108.
- Bret, A., A. Stockem, R. Narayan, and L. O. Silva (2014), *Physics of Plasmas* **21** (7), 072301.
- Capdessus, R., E. d'Humières, and V. T. Tikhonchuk (2012), *Physical Review E* **86**, 036401.
- Chen, M., A. Pukhov, T.-P. Yu, and Z.-M. Sheng (2011), *Plasma Physics and Controlled Fusion* **53** (1), 014004.
- Denavit, J. (1992), *Physical Review Letters* **69** (21), 3052.
- Duclous, R., J. G. Kirk, and A. R. Bell (2011), *Plasma Physics and Controlled Fusion* **53** (1), 015009.
- Elkina, N. V., A. M. Fedotov, I. Y. Kostyukov, M. V. Legkov, N. B. Narozhny, E. N. Nerush, and H. Ruhl (2011), *Physical Review Special Topics - Accelerators and Beams*, vol. 14, Issue 5, id. 054401 **14** (5), 054401.
- Esirkepov, T., M. Borghesi, S. V. Bulanov, G. Mourou, and T. Tajima (2004), *Physical Review Letters* **92** (17), 175003.
- Fedotov, A. M., N. B. Narozhny, G. Mourou, and G. Korn (2010), *Physical Review Letters* **105** (8), 080402.
- Fox, W., G. Fiksel, A. Bhattacharjee, P.-Y. Chang, K. Geraschewski, S. X. Hu, and P. M. Nilson (2013), *Physical Review Letters* **111**, 225002.
- Gonoskov, A., I. Gonoskov, C. Harvey, A. Ilderton, A. Kim, M. Marklund, G. Mourou, and A. Sergeev (2013), *Physical Review Letters* **111**, 60404.
- Ji, L., A. Pukhov, and B. Shen (2014a), *New Journal of Physics* **16** (6), 063047.
- Ji, L. L., A. Pukhov, I. Y. Kostyukov, B. F. Shen, and K. Akli (2014b), *Physical Review Letters* **112** (14), 145003.
- Ji, L. L., A. Pukhov, E. N. Nerush, I. Y. Kostyukov, B. F. Shen, and K. U. Akli (2014c), *Physics of Plasmas* **21** (2), 023109.
- Kar, S., K. F. Kakolee, M. Cerchez, D. Doria, A. Macchi, P. McKenna, D. Neely, J. Osterholz, K. Quinn, B. Ramakrishna, G. Sarri, O. Willi, X. H. Yuan, M. Zepf, and M. Borghesi (2013), *Plasma Physics and Controlled Fusion* **55** (12), 124030.
- King, B., and A. Di Piazza (2014), *The European Physical Journal Special Topics* **223** (6), 1063.
- Kirk, J. G., A. R. Bell, and C. P. Ridgers (2013), *Plasma Physics and Controlled Fusion* **55** (9), 095016.
- Kruer, W. L., E. J. Valeo, and K. G. Estabrook (1975), *Physical Review Letters* **35** (16), 1076.
- Macchi, A., M. Borghesi, and M. Passoni (2013), *Reviews of Modern Physics* **85**, 751.
- Macchi, A., F. Cattani, T. V. Liseykina, and F. Cornolti (2005), *Physical Review Letters* **94**, 165003.
- Mourou, G., and T. Tajima (2014), *The European Physical Journal Special Topics* **223** (6), 979.
- Nakamura, T., J. K. Koga, T. Z. Esirkepov, M. Kando, G. Korn, and S. V. Bulanov (2012), *Physical Review Letters* **108** (19), 195001.
- Narozhny, N. B., and A. M. Fedotov (2014), *The European Physical Journal Special Topics* **223** (6), 1083.
- Naumova, N., T. Schlegel, V. T. Tikhonchuk, C. Labaune, I. V. Sokolov, and G. Mourou (2009), *Physical Review Letters* **102** (2), 025002.
- Nerush, E. N., V. F. Bashmakov, and I. Y. Kostyukov (2011a), *Physics of Plasmas* **18** (8), 083107.
- Nerush, E. N., and I. Y. Kostyukov (2011), *Nuclear Instruments and Methods in Physics Research A* **653** (1), 7.
- Nerush, E. N., I. Y. Kostyukov, A. M. Fedotov, N. B. Narozhny, N. V. Elkina, and H. Ruhl (2011b), *Physical Review Letters* **106** (3), 035001.
- Nerush, E. N., I. Y. Kostyukov, L. Ji, and A. Pukhov (2014), *Physics of Plasmas* **21**, 013109.
- Palmer, C. A. J., N. P. Dover, I. Pogorelsky, M. Babzien, G. I. Dudnikova, M. Ispiriyani, M. N. Polyanskiy, J. Schreiber, P. Shkolnikov, V. Yakimenko, and Z. Najmudin (2011), *Physical Review Letters* **106**, 014801.
- Palmer, C. A. J., J. Schreiber, S. R. Nagel, N. P. Dover, C. Bellei, F. N. Beg, S. Bott, R. J. Clarke, A. E. Dangor, S. M. Hassan, P. Hilz, D. Jung, S. Kneip, S. P. D. Mangles, K. L. Lancaster, A. Rehman, A. P. L. Robinson, C. Spindloe, J. Szerypo, M. Tatarakis, M. Yeung, M. Zepf, and Z. Najmudin (2012), *Physical Review Letters* **108**, 225002.
- Ridgers, C. P., C. S. Brady, R. Duclous, J. G. Kirk, K. Bennett, T. D. Arber, and A. R. Bell (2013), *Physics of Plasmas*, Volume 20, Issue 5, pp. 056701-056701-6 (2013). **20**, 056701.
- Ridgers, C. P., C. S. Brady, R. Duclous, J. G. Kirk, K. Bennett, T. D. Arber, A. P. L. Robinson, and A. R. Bell (2012), *Physical Review Letters* **108** (16), 165006.
- Robinson, A. P. L., P. Gibbon, M. Zepf, S. Kar, R. G. Evans, and C. Bellei (2009), *Plasma Physics and Controlled Fusion* **51** (2), 024004.
- Schlegel, T., N. Naumova, V. T. Tikhonchuk, C. Labaune, I. V. Sokolov, and G. Mourou (2009), *Physics of Plasmas*, Volume 16, Issue 8, pp. 083103-083103-16 (2009). **16**, 083103.
- Silva, L. O., R. A. Fonseca, J. W. Tonge, J. M. Dawson, W. B. Mori, and M. V. Medvedev (2003), *The Astrophysical Journal Letters* **596** (1), 4.
- Tamburini, M., T. V. Liseykina, F. Pegoraro, and A. Macchi (2012), *Physical Review E* **85**, 016407.
- Tamburini, M., F. Pegoraro, A. D. Piazza, C. H. Keitel, and A. Macchi (2010), *New Journal of Physics* **12** (12), 123005.
- Wilks, S. C., W. L. Kruer, M. Tabak, and A. B. Langdon (1992), *Physical Review Letters* **69** (9), 1383.